Development of XAFS theory†

A. L. Ankudinov* and J. J. Rehr

Department of Physics, Box 351560, University of Washington, Seattle, WA 98195, USA. E-mail: alex@phys.washington.edu

A major goal of theoretical simulations of X-ray absorption fine structure (XAFS) is to provide calculations for the interpretation and analysis of experimental data in terms of geometrical and electronic information. The extended region or EXAFS (50–2000 eV above an absorption edge) contains geometric information about the pair distribution function, *i.e.* distances to the nearest neighbors and their orientation. The theory of EXAFS is now well understood and has been recently reviewed [Rehr & Albers (2000). *Rev. Mod. Phys.* **72**, 621–654]. The near-edge region (0–50 eV above the edge) or X-ray absorption near-edge structure (XANES) probes the states just above the Fermi level, and contains important electronic information, *e.g.* the electronic density of states (DOS). This data can be used to obtain the number of electrons or holes in the electronic configuration and spin and orbital moments on a particular atom *via* sum rules. XANES calculations with our *ab initio* code *FEFF8* [Ankudinov *et al.* (1998). *Phys. Rev. B*, **58**, 7565–7576] usually give semi-quantitative agreement with experiment, and permits the interpretation of XANES in terms of DOS. However, fully quantitative calculations remain a challenge. Several effects still need to be considered to treat the XANES region. These include non-spherical parts of the scattering potential and many-body effects such as multi-electron excitations, core-hole effects and local field effects (screening of the X-ray field).

Keywords: XAFS; X-ray absorption; XANES.

The theory of X-ray absorption fine structure (XAFS) is already more than 70 years old. A detailed review of the first 40 years is given by Stumm von Bordwehr (1989) but here we focus on developments essential for the XANES region. The theory was first developed by Kronig (1931, 1932) immediately after the development of quantum mechanics. Thus according to Fermi's Golden rule, the X-ray absorption cross section is proportional to the square of the matrix element between initial and final states,

$$\sigma(E) \propto \sum_f |\langle \Psi_i | \vec{\varepsilon} \cdot \vec{r} | \Psi_f \rangle|^2 \, \delta\big[E - \big(E_f - E_i\big)\big], \qquad (1)$$

where the initial state i is an occupied deep core-hole state, and final state f is unoccupied. Assuming that the matrix element is a smooth function of energy, X-ray absorption is directly related to the density of states $\sigma(E) = M(E)^2 \rho_\ell(E)$, where the final-state angular momentum ℓ is determined by the dipole selection rules $\ell = \ell_i \pm 1$. This relationship serves as a basis of the first theoretical interpretation of X-ray absorption fine structure by Kronig (1931). Thus one might think that in crystals the features in XAFS are due to features in the band structure, such as Van Hove singularities. This became known as the long-range order (LRO) interpretation. A second paper on the fine structure in molecules was also written by Kronig (1932). It is based on the multiple-scattering (MS) representation of the final-state density of states. In the plane-wave limit one obtains the fine structure as a sum of terms χ^N, where each term represents the $(N-1)$th-order MS contribution (Rehr & Albers, 1990),

$$\sigma(E) = \sigma_0(E)\left[1 + \mathrm{Im}\exp\big(2i\delta_\ell\big) \sum_{N=2}^{\infty} \chi^N(E)\right], \qquad (2)$$

$$\chi^N = \big(\hat{R}_1 \cdot \hat{R}_N\big) \prod_{j=1}^{N} \frac{\exp(ikR_j)}{kR_j} \prod_{j=1}^{N-1} f_j(\Theta_j). \qquad (3)$$

Here $f_j(\Theta_j)$ is the plane-wave scattering amplitude at atom number j, and each term $\exp(ikR)/(kR)$ represents the propagation of a plane wave between two atoms, where $R_j = |\vec{R}_j|$ and the vector $\vec{R}_j$ goes from atom $j-1$ to atom j. For X-ray absorption, atom number N is equivalent to atom number 0 at the absorbing atom. Each Nth-order path has $N-1$ scattering events and N propagations from site to site. Thus XAFS can be viewed as a quantum interference effect on the photoelectron wavefunction. The wave scattered from the neighbors can increase or decrease absorption, depending on it's constructive or destructive interference with outgoing photoelectron wavefunction. The photoelectron wavevector k is directly connected to the X-ray photon energy $k^2/2 \simeq E - E_\mathrm{F}$ (in atomic units), and hence one expects an oscillation with a period of $2kR = 2\pi$ for a single scattering contribution. Thus roughly if one measures the maximum absorption at k_1 and k_2 for a diatomic molecule, the interatomic distance is about $R = \pi/(k_2 - k_1)$. This is the short-range-order theory. The first calculations of the XAFS were made by Hartree *et al.* (1934) shortly after short-range-order theory was developed. He showed that there is a significant fine structure for the $GeCl_4$ molecule, and he also suggested that it can be used to determine the distances. This type of distance determination is known now as extended XAFS (EXAFS) analysis.

The question of whether the observed XAFS is dominated by long-range order (electronic structure features) or short-range order (SRO) (geometric structure) puzzled researchers for about 40 years. However, the LRO theory suffered an almost fatal blow from the paper by Sayers *et al.* (1971), which showed that the peaks in the EXAFS Fourier transform of a Ge crystal correspond to the interatomic distances in Ge. Shortly after, however, Schaich (1973) showed that theoretically LRO and SRO are formally equivalent, in that both can be obtained within MS theory. The SRO theory corresponds to a weak scattering limit, where the scattering amplitude is small and the high-order terms in equation (2) are negligible. The LRO theory corresponds to the case of strong scattering, *i.e.* when very many terms in equation (2) are needed.

We demonstrate this separation in Fig. 1, which shows the calculation of the boron K-edge XAFS using the full MS technique (Ankudinov *et al.*, 1998) (LRO) and using the path-expansion method (Rehr & Albers, 2000) (SRO). The energy scale is shifted up by 10 eV compared with Fig. 1 of Ankudinov *et al.* (1998), where we shifted calculations to match the most intensive peak. Also the present calculations were performed neglecting the self-energy losses, to see larger fine structure in the EXAFS region. It is clear that the two results for the XAFS agree well above 50 eV from the edge, which is typically taken as the separation between the XANES and EXAFS region. Below that energy, path expansion does not converge. It should not converge, if the largest eigenvalue of the GT matrix (shown by dashes in Fig. 1) is larger than 1. This eigenvalue corresponds to the ratio between the $(N+1)$th and Nth-order scattering contributions in equation (2) for high N, and it is larger than 1 up to 70 eV above the edge. The path expansion seems to work between 50 and 70 eV above the edge probably due to cancellation of high N

† Presented at the 'XIV Russian Synchrotron Radiation Conference SR2002', held at Novosibirsk, Russia, on 15–19 July 2002.

terms in the series. The powerful Lanczos algorithm was first applied for the X-ray absorption calculation using continued fraction expansion by Filipponi (1991). The iterative Lanczos techniques (Ankudinov *et al.*, 2002) of the full MS calculations estimate the error at each iteration, and the iteration number corresponds directly to the number of terms used in equation (2). The MS order needed to converge to within 1% is also shown in Fig. 1 by dots. The maximum $N = 8$ was used in the path expansion calculation, and therefore once the MS order required becomes larger than eight then one observes a failure of the path expansion. Interestingly, MS order has a fine structure which correlates with XAFS, depending on whether the interference between paths is constructive or destructive.

The most important information that one obtains from EXAFS is information about the path distribution function (PDF), which is clear from a Fourier transform of the EXAFS signal. The lengths of the paths that give a major contribution to the EXAFS signal serve as a constraint to building a geometrical model of the crystal or molecule. Numerous applications of the EXAFS method to obtain the PDF for liquids have been recently reviewed (Filipponi, 2001). The major advantages of EXAFS over a PDF analysis of X-ray diffraction are the element specificity and the presence of MS paths (Dimitrov *et al.*, 1998). For example, buckling distortions are practically invisible in diffraction, but have a significant impact on EXAFS (Dimitrov *et al.*, 1998; Frenkel *et al.*, 1994). The success of EXAFS theory and analysis is due to the fact that the propagation of a photoelectron at high energy is not very sensitive to the fine details of potentials and behaves almost as a free electron with weak scattering. This allowed the creation of accurate computer codes to aid the analysis, and obtain geometrical information to very high accuracy (typically of order 0.01 Å).

Current development in XAFS theory are focused on the XANES region. This region can be used to find electronic structure above the Fermi level. The relationship between XAFS and DOS is most vividly expressed within MS theory (Nesvizhskii *et al.*, 2001) as

$$\sigma(E) = [\,\rho_0(E)/\mu_0(E)]\,\rho_\ell(E). \qquad (4)$$

In earlier theories this ratio was typically taken as a constant, but now it's energy dependence can be calculated (Nesvizhskii *et al.*, 2001).

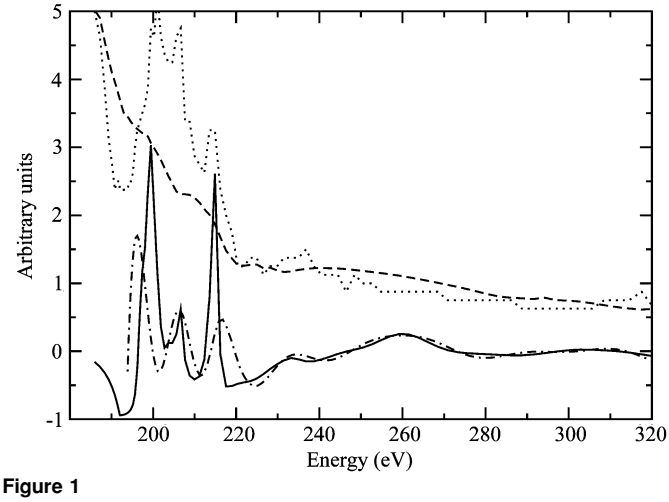

Figure 1
Separation between the EXAFS (SRO) and XANES (LRO) regions for the boron *K*-edge of cubic BN. The path expansion calculation (dot–dashed line) fails to converge to the full MS result (solid line) below 50 eV above the edge. It is expected to fail once the largest eigenvalue (dashed line) is larger than unity. MS order (dots), needed to converge to within 1% using the Lanczos iterative technique (reduced by a factor of eight to show on the same plot).

Thus one can investigate detailed electronic structure with XANES. For example, the excited-state energy levels can exhibit splittings under distortion, which can be used to find geometrical information from XANES (Frenkel *et al.*, 2000; Durham *et al.*, 1981; Benfatto & Della Longa, 2001). Also for integrated intensities one can obtain sum rules within single-particle theory (Ankudinov & Rehr, 1995) or within atomic theory that includes many-body effects (Thole *et al.*, 1992; Carra *et al.*, 1993). These sum rules show that from the integrated intensity one can extract the number of holes, spin and orbital moments, and expectation values from a few other operators. Such operators are of key interest in chemistry, since the number of holes is directly connected to the electronic configuration of a particular atom. They are also important in studies of magnetism, since one can separate for each atomic type the spin and orbital contributions to the total magnetization.

Compared with the EXAFS region, where one can use overlapped atomic potentials to calculate scattering amplitude and phases, in the XANES region, even within single electron theory, there are additional complications. There the photoelectron is more sensitive to the details of potential, and one needs to calculate the potential self-consistently and often include non-spherical contributions (Foulis *et al.*, 1990). Both effects can be neglected in EXAFS. Also the use of sum rules and the construction of energy-level diagrams from XANES is complicated by several factors. The most serious one is the fact that a core-hole is present in the final state, which modifies the scattering potential. Consideration of this effect led to the Mahan–Nozieres-de Dominici theory of edge singularities (Nozieres & De Dominicis, 1969). Actually, owing to final core-hole lifetime the singularity should disappear, but still might lead to significant enhancement (*i.e.* excitonic effect due to Coulomb interaction between core-hole and photoelectron) and/or reduction (Anderson orthogonality catastrophe) near the absorption edge. Currently, significant progress has been made in the calculation of excitonic effects in the optical region (Rohlfing & Louie, 2000). This has also lead to progress with similar calculation for the X-ray regime (Soininen & Shirley, 2001). Another effect which strongly affects the XANES calculation at low X-ray energies (*i.e.* below 1000 eV) is the dynamic screening of the X-ray electric field (Zangwill & Soven, 1980). Thus the effective screened (and not bare external) electric field enters the calculation of the matrix element. This strongly affects the $L2/L3$ branching ratio for $3d$ transition metals (Schwitalla & Ebert, 1998).

The excitonic interaction and dynamic screening affect how one should extract information from XANES. First, owing to excitonic effects, the energy levels are expected to shift down near the Fermi level, and this shift is much smaller at high energies. Dynamic screening affects mostly the atomic matrix elements (μ_0), and should be included in the calculation of ρ_0/μ_0. Thus one obtains the ground-state density of states if the matrix element is calculated including dynamic screening and one undoes the shift caused by the excitonic interaction. Yet an additional complication arises due to the possibility of multiplet splitting (de Groot, 1994), *e.g.* the energy levels of the final $\underline{c}d^{n+1}$ configuration may differ from the energy levels of the d^n ground-state configuration. Thus for large multiplet splitting the energy levels should be drawn separately for the ground state and excited states with core-hole. On the other hand, this splitting is typically of the order of a few eV and mostly should not affect the extraction of hole counts and spin/orbital moments.

In conclusion, the EXAFS region is predominately governed by short-range-order theory and contains geometrical information about a few most important scattering paths. Extraction of this information is facilitated by theoretical calculations of individual path-scattering

amplitude and phases. Current developments in XAFS theory are focused on the XANES region, which is predominately governed by long-range-order theory (strong scattering), and contains electronic structure information about energy levels, number of holes, spin and orbital moments. In general, more accurate potentials are required: self-consistency and non-spherical contributions are important. Many-body effects (excitonic interaction, dynamic screening of X-ray field, multiplet splittings) may also significantly affect the extraction of electronic information.

This work was supported by DOE grant DE-FG03-97ER45623, and was facilitated by the DOE Computational Materials Science Network.

References

Ankudinov, A. L. & Rehr, J. J. (1995). *Phys. Rev. B*, **51**, 1282–1285.
Ankudinov, A. L., Bouldin, C. E., Rehr, J. J., Sims, J. & Hung, H. (2002). *Phys. Rev. B*, **65**, 104107.
Ankudinov, A. L., Ravel, B., Rehr, J. J. & Conradson, S. D. (1998). *Phys. Rev. B*, **58**, 7565–7576.
Benfatto, M. & Della Longa, S. (2001). *J. Synchrotron Rad.* **8**, 1087–1094.
Carra, P., Thole, B. T., Altarelli, M. & Wang, X. (1993). *Phys. Rev. Lett.* **70**, 694–697.
Dimitrov, D. A., Ankudinov, A. L., Bishop, A. R. & Conradson, S. D. (1998). *Phys. Rev. B*, **58**, 14227–14237.
Durham, P. J., Pendry, J. B. & Hodges, C. H. (1981). *Solid State Commun.* **38**, 159–162.
Filipponi, A. (1991). *J. Phys. Condens. Matter*, **3**, 6489–6507.
Filipponi, A. (2001). *J. Phys. Condens. Matter*, **13**, R23–R60.
Foulis, D. L., Pettifer, R. F., Natoli, C. R. & Benfatto, M. (1990). *Phys. Rev. A*, **41**, 6922–6927.
Frenkel, A. L., Korshin, G. V. & Ankudinov, A. L. (2000). *Environ. Sci. Technol.* **34**, 2138–2142.
Frenkel, A., Stern, E. A., Voronel, A., Qian, M. & Newville, M. (1994). *Phys. Rev. B*, **49**, 11662–11674.
Groot, F. M. F. de (1994). *J. Electron Spectrosc.* **67**, 529–622.
Hartree, D. R., Kronig, R. & Petersen, H. (1934). *Physica*, **1**, 895–924.
Kronig, R. (1931). *Z. Phys.* **70**, 317–323.
Kronig, R. (1932). *Z. Phys.* **75**, 468–475.
Nesvizhskii, A. I. Ankudinov, A. L. & Rehr, J. J. (2001). *Phys. Rev. B*, **63**, 094412.
Nozieres, P. & De Dominicis, C. T. (1969). *Phys. Rev.* **178**, 1097–1107.
Rehr, J. J. & Albers, R. C. (1990). *Phys. Rev. B*, **41**, 8139–8149.
Rehr, J. J. & Albers, R. C. (2000). *Rev. Mod. Phys.* **72**, 621–654.
Rohlfing, M. & Louie, S. G. (2000). *Phys. Rev. B*, **62**, 4927–4944.
Sayers, D. E., Stern, E. A. & Lytle, F. W. (1971). *Phys. Rev. Lett.* **27**, 1204–1207.
Schaich, W. L. (1973). *Phys. Rev. B*, **8**, 4028–4032.
Schwitalla, J. & Ebert, H. (1998). *Phys. Rev. Lett.* **80**, 4586–4589.
Soininen, J. A. & Shirley, E. L. (2001). *Phys. Rev. B*, **64**, 165112.
Stumm von Bordwehr, R. (1989). *Ann. Phys. Fr.* **14**, 377–466.
Thole, B. T., Carra, P., Sette, F. & van der Laan, G. (1992). *Phys. Rev. Lett.* **68**, 1943–1946.
Zangwill, A. & Soven, P. (1980). *Phys. Rev. A*, **21**, 1561–1572.